Chapter 3

Structural and Magnetic Properties of Quasi-One-dimensional doped $LiCuVO_4$

3.1 Introduction

Dimensionality and the spin magnitude *S* play important roles in the physical properties of interacting systems because quantum fluctuation is affected significantly by them. Quantum fluctuation enhanced both by geometric frustration and by spin frustration may destroy antiferromagnetic (AFM) order and yield a rich variety of ground states, novel excitations, and exotic behaviours that currently attract much attention. As a matter of fact, low dimensional quantum magnets have become one of the most important topics because of various interesting quantum magnetic phenomena.[1-5]It has motivated us to work on phenomena principally governed by quantum effects in other classes of low dimensional systems. The 1D cuprate $LiCuVO_4$ with spin S=1/2 (in $x^2–y^2$ orbital) has only one crystallographically distinct Cu site[6] and it crystallizes in an orthorhombic distorted inverse spinel structure, in which the non magnetic V^{5+} ($3d^0$) ions occupy the tetrahedral sites, whereas Li^+ and Cu^{2+} are arranged in an ordered way on the octahedral sites.[7] Both LiO_6 and CuO_6 octahedra form independent chains along the c direction. The chains consist of edge-sharing octahedra with two nearly rectangular Cu-O-Cu super-exchange bonds between two Cu-ions as schematically shown in Fig. 3.1.[8,9] Moreover, for this system, the exchange interaction between the nearest-neighbor Cu^{2+} ions through Cu-O-Cu exchange path is rather weak, as expected for the Cu-O-Cu angle close to 90^0 ($\sim 95^0$) or even weaker than the next nearest-neighbor interaction[10-12] suggesting the effects of the magnetic frustration are significant in its magnetic properties. The magnetic susceptibility of $LiCuVO_4$ exhibits a broad maximum at T_M ~28 K and is described by a Heisenberg antiferromagnetic chain model with spin exchange parameter of -45 K.[13] It has also been established that $LiCuVO_4$ forms an incommensurate magnetic superstructure (0, 0.532, 0) below 2.1K.[14] In this commensurate approximation, each CuO_2 chain in the magnetic superstructure of $LiCuVO_4$ contains four Cu^{2+} ions per magnetic unit cell. The associated spin arrangement shows that the antiferromagnetic next nearest neighbour (NNN) spin exchange interaction J_2 (<0) is much stronger in magnitude than the ferromagnetic nearest neighbour (NN) spin exchange interaction J_1. This also has recently been verified by Kremer,[15]who fitted the magnetic susceptibility of $LiCuVO_4$ using the high-temperature series expansion formula ofBühler et al.[16] and they found that the value of J_1 variesfrom 3.0 to 12.7K and that of J_2 from -43.2 to – 48.5K. Moreover, the interchain spin exchange of $LiCuVO_4$ is much weaker than the intrachain spin exchange such that the occurrence

of the magnetic superstructure in $LiCuVO_4$ must largely be driven by the tendency for each CuO_2 chain to have its NNN spins order antiferromagnetically. However, Sirker[17] reported a strikingly different set of the spin exchanges ($J_1 \approx 7.8$ meV with $|J_2/J_1| \approx 0.5$). Subsequently Enderle et al. from their neutron scattering and magnetization data led to different sets of spin exchange constants for $LiCuVO_4$.[18]

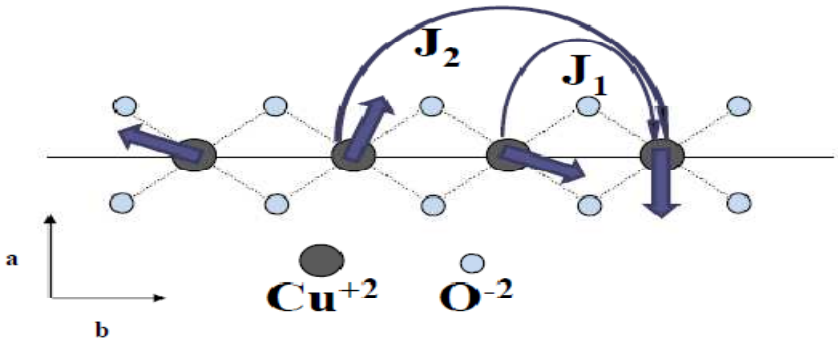

(a)

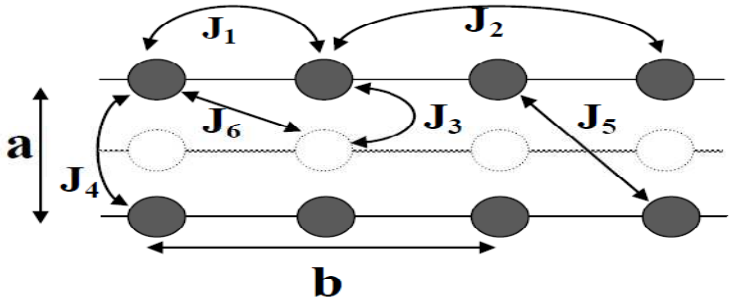

(b)

Figure 3.1*Schematic diagram of (a) intrachain interaction path between Cu^{2+} in CuO_4 unit and (b) interaction path between Cu^{2+} in ab plane (solid line) and plane shifted by c/2 (dashed line) of $LiCuVO_4$.*

To obtain insights into the nature of the puzzling properties of the S=1/2 spin-chain compound $LiCuVO_4$, we have investigated the magnetic properties of the Co-, Zn- and Mn-doped compound. We have doped Zn, Co and Mn separately on the Cu site. Also, we have attempted to resolve the aforementioned controversy regarding the relative magnitudes of J_1 and J_2 in $LiCuVO_4$. We have also seen the effect of different doping on the exchange interactions J_1 and J_2. The interchain exchange interactions (J_4 and J_5 in 18) have also been considered. It has been observed with doping the interchain exchange

interactions play dominant role in the magnetic property. Zn effect is interesting since it is a non-magnetic ion and therefore, it will have appreciable effect on the exchange interaction. Co^{2+} is a magnetic ion with spin quantum number 3/2. On the other hand the Mn-doping may also play a major role by inducing ferromagnetism as has been observed in dilute magnetic semiconductor.[19] To the best of our knowledge this is the first time the evolution of the ferromagnetic ordering with doping in this low dimensional $LiCuVO_4$ has been shown.

3.2 Experimental

The polycrystalline samples were prepared by solid-state reaction from high purity Li_2CO_3, CuO, V_2O_5, ZnO, Co_3O_4 and MnO powders. Powders were taken in stoichiometric ratio. The mixture was ground and pressed into pellets, sintered in air at 550^0C for 48 hours with intermediate grindings and furnace cooled. The process of synthesis is given by below flow chart diagram.

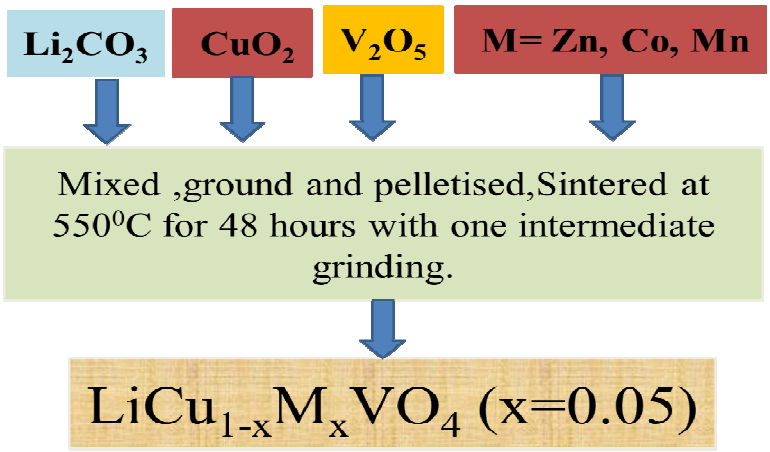

The X-ray powder diffraction has been characterized from Rigaku MiniFlex II DEXTOP X-ray Diffractometer with Cu-Kα radiation [Filtered source] and sample mounted horizontly. Magnetic measurement was done using MPMS SQUID (Quantum Design) magnetometer with the bulk samples. Data were collected upon warming up the sample. Magnetization as a function of temperature has been measured at different magnetic field. The Neutron diffraction measurement was performed on the neutron powder diffractometer (PD2) at Bhabha Atomic Research Centre, Mumbai, India using neutrons of wavelength, λ=1.2443Å. X-ray photoemission spectroscopic (XPS) measurement was performed on the samples using a Specs (Germany) system with a hemispherical energy analyser. A non-monochromatic Mg Kα

X-ray (1253.6 eV) was used as the excitation source operated at 10 kV and with an anode current 17 mA. The residual pressure of the system was ~10^{-9} mbar.

3.3 Results & Discussion

3.3.1 X-Ray Diffraction Study

Figure 3.2 shows X-ray Diffraction pattern of $LiCu_{0.95}M_{0.05}VO_4$ (M=Zn, Co, Mn) samples which clearly indicates the single phase [Consistent with card no 18-0726].

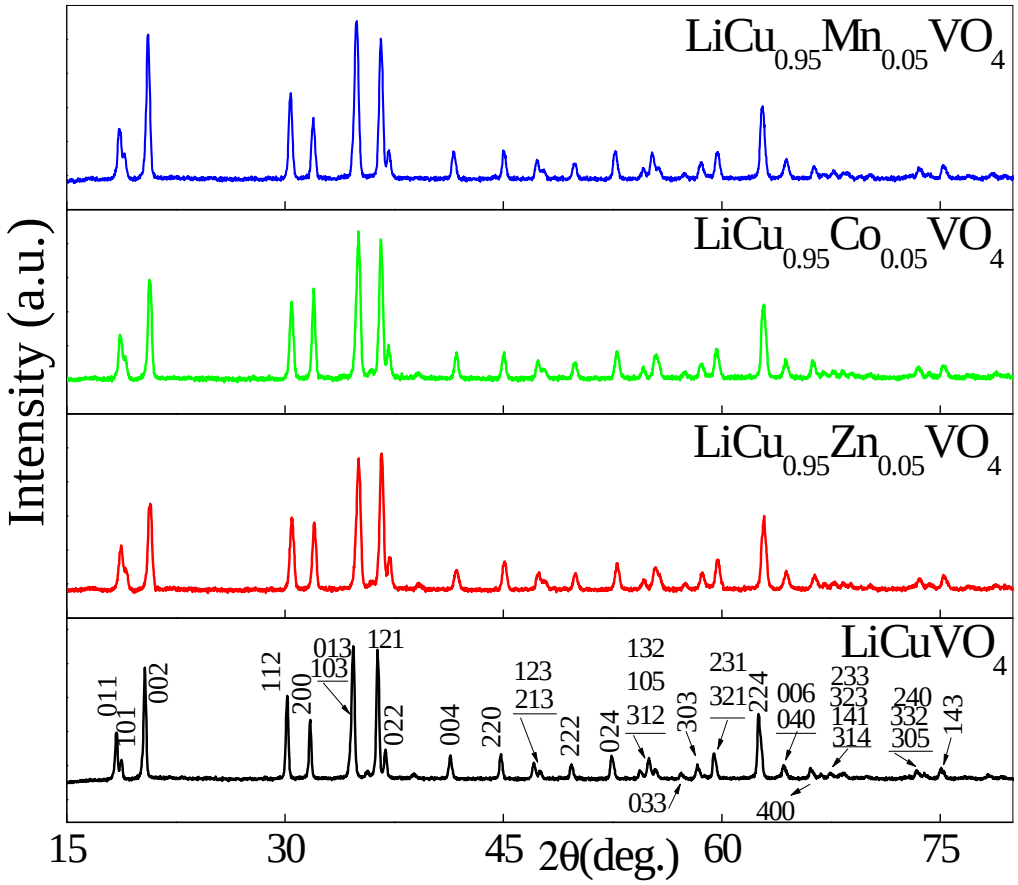

Figure 3.2: *X-ray Diffraction patterns of $LiCuVO_4$, $LiCu_{0.95}Zn_{0.05}VO_4$, $LiCu_{0.95}Co_{0.05}VO_4$, and $LiCu_{0.95}Mn_{0.05}VO_4$ samples.*

3.3.2 Study of Magnetic Property

3.3.2.1 Analysis of Magnetization (M) Vs Temperature (T)

Fig. 3.3 shows the Field cooled (FC) dc-susceptibility (χ=M/H, M is the magnetization) as a function of temperature at magnetic fields H= 100 Oe (inset: at magnetic field 5000 Oe) for doped and undoped $LiCuVO_4$ samples.

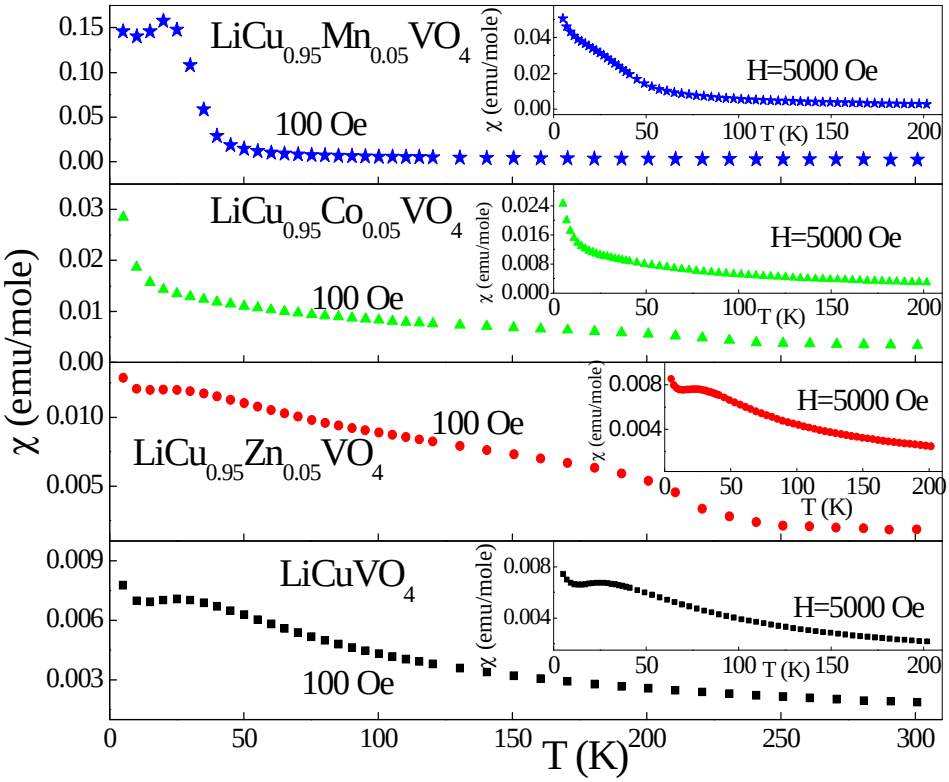

Figure 3.3: *Magnetic susceptibility vs Temperature curve, χ(T), of$LiCuVO_4$, $LiCu_{0.95}Zn_{0.05}VO_4$, $LiCu_{0.95}Co_{0.05}VO_4$ and $LiCu_{0.95}Mn_{0.05}VO_4$ samples at 100 Oe (Inset: χ(T) at 5000 Oe).*

For $LiCuVO_4$ as temperature decreases the susceptibility passes through a wide peak at T_m~26K and then increases somewhat at 10K. The behavior is consistent with those already reported.[13, 20, 21] It is observed that with doping of Zn, χ(T) behavior remain same except slight increased value of susceptibility and also an appreciable enhancement is occurred around 250K. At low temperature the Co-doped sample shows a sharp increase without any peak. Co-doping sample also shows a small enhancement around 242 K. The χ(T) curve of Mn-doped $LiCuVO_4$ also shows a broad peak around 21K. As the magnetic field increases the broad peak diminishes but the signature remains there even at higher magnetic field (inset in Fig. 3.3).

3.3.2.2 Modified Curie-Weiss (MCW) Fitting Analysis

Due to weak magnetic interaction in $LiCuVO_4$, the magnetic susceptibility at high temperature is a measurement of the concentration of the magnetic copper ions, and can determine the effectiveness of chemical doping. It is observed with doping of different ions (magnetic/nonmagnetic) the magnetic moment increases. The effect of doping can

also be estimated quantitatively by the calculation of the effective moment. In order to study the doping effect we have fitted the magnetic susceptibility data to the the theoretical susceptibilities given by

$$\chi_{th} = \chi_{spin}(T) + \chi_0 \quad (1)$$

where the spin susceptibility, χ_{spin}(T)can be described by Curie-Weiss susceptibility

$$\chi_{spin} = C/(T+\theta) \quad (2)$$

where C is the curie constant and θ is the Weiss constant.

At high temperatures where the spin susceptibility is small enough, the fitting analysis of the observed magnetic susceptibility is significantly influenced by the sign of the temperature independent magnetic susceptibility χ_0. $\chi_0$is given by $\chi_0 = \chi_{dia} + \chi_{VV}$; where χ_{dia} is the diamagnetic contribution from the closed electron shell ions and χ_{VV} is the temperature-independent Van Vleck contribution. In order to extract the values ofχ_0 and θ for all the samples the high temperature range of DC susceptibility were fitted [Fig. 3.4] to the modified Curie-Weiss law, Eq (1). The obtained values of χ_0 and θ are shown in Table3.1.

Table 3.1

J_1 and J_2 values obtained from HTSE fitting of magnetic susceptibility dataof$LiCuVO_4$, $LiCu_{0.95}Zn_{0.05}VO_4$, $LiCu_{0.95}Co_{0.05}VO_4$ and $LiCu_{0.95}Mn_{0.05}VO_4$samples in temperature range 50–300 K. $\chi 0$ and θ values obtained by fitting with modified Curie–Weiss law in the temperature region 150–300 K.

Sample/Parameter	$LiCuVO_4$	$LiCu_{0.95}Zn_{0.05}VO_4$	$LiCu_{0.95}Co_{0.05}VO_4$	$LiCu_{0.95}Mn_{0.05}VO_4$
J_1/k_B (K)	13.23	4.9	11.84	16.15
$\alpha = J_2/J_1$	-5.37	-13.19	-6.53	-0.4
χ0 (HTSE fit)	-4.87E-5	4.69E-05	6.90E-04	2.12E-04
θ (K) (HTSE fit)	-28.91	-29.87	-32.74	4.85
χ0 (CW fit)	-4.48E-5	-29.78E-5	-12.767E-5	12.16E-5
θ (K) (CW fit)	-25.2	-29.8	-39.24	4.5

The effective magnetic moment μ_{eff} can be obtained by evaluating the relation:

$$C=N\mu_{eff}^2/3k_B$$

Where N is the number density of magnetic ions per unit gram, k_B is the Boltzmann's constant. Since the Zn, Co and Mn are doped in the Cu^{2+} site the theoretical expected magnetic moment of Zn-doped and Mn-doped $LiCuVO_4$ can be calculated from the equation: $\mu_{eff}=g[S_{avg}(S_{avg}+1)]^{1/2}$ where g factor is 2.26.[4]The effective moments from the Curie constant are calculated to be 2.01μ_B, 2.26μ_B, 2.42μ_B and 2.06μ_B respectively, for

undoped, Zn-doped, Co-doped and Mn-doped samples. The theoretical values of effective moments for $LiCuVO_4$, $LiCu_{0.95}Zn_{0.05}VO_4$, $LiCu_{0.95}Co_{0.05}VO_4$ and $LiCu_{0.95}Mn_{0.05}VO_4$ respectively, are $1.957\mu_B$, $1.89\mu_B$, $2.09\mu_B$ and $2.21\mu_B$ which are in good agreement with the experimentally observed values. But for Zn-doped sample the values differ much. In actual case Zn is nonmagnetic and therefore with doping of Zn the magnetic moment should decrease as has been observed for the hole-doped $LiCuVO_4$.[12]

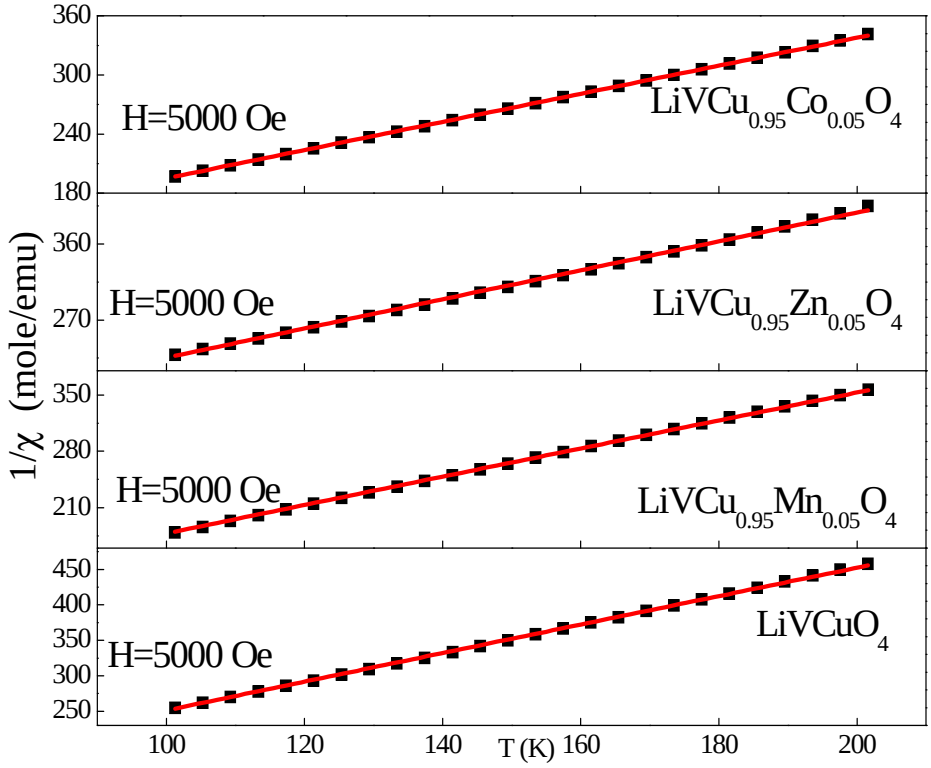

Figure 3.4: *Modified Curie-Weiss Law fitting of the χ(T) data of $LiCuVO_4$, $LiCu_{0.95}Zn_{0.05}VO_4$, $LiCu_{0.95}Co_{0.05}VO_4$ and $LiCu_{0.95}Mn_{0.05}VO_4$ samples in the temperature range 100K-200K.*

But in the present investigation it has been observed that with 5% Zn doping at low temperature the magnetization value increases slightly.Moreover, with Zn doping the AFM correlation length of magnetic Cu^{2+} increases leading to the increase of θ value. The increase in the μ_{eff}might be due the change of the canting angle of the Cu spins. Co ion also increases the AFM correlation length as with Co doping θ value increases. Moreover, the spin quantum number of Co^{2+} is larger (3/2) than that of Cu^{2+} and as a matter of fact the magnetization value increases with doping of Co. It is observed from the Curie-Weiss fitting for the Mn-doped sample that θ value becomes positive which is the indication of the induced of ferromagnetism.

3.3.2.3 High-Temperature Series expansion (HTSE) Analysis of the Magnetic Susceptibility

But in the present investigation it has been observed that with 5% Zn doping at low temperature the magnetization value increases slightly. Moreover, Zn doping increases the AFM correlation length of magnetic Cu^{2+} leading to the increase of θ value. The increase in the μeff might be due to the change of the canting angle of the Cu spins. Co ion also increases the AFM correlation length as with Co doping θ valueincreases. Moreover, the spin quantum number of Co^{+2} is larger (3/2) than that of Cu^{+2} and as a matter of fact the magnetization value increases with doping of Co. It is observed from the Curie–Weiss fitting for the Mn-doped sample that θ value becomespositive which is the indication of the induced ferromagnetism. Moreover, χ_{spin} can also be described by a high-temperature series expansion (HTSE) of the magnetic susceptibility for a frustrated S=1/2 Heisenberg chain defined by J_1 and J_2. For sucha chain, the HTSE of the magnetic susceptibility is expressed as[15]

$$\chi_{spin} = \left(1/T\right) \sum c_{n,k}\, \alpha^k \left(-J_1/k_B T\right)^n \qquad (3)$$

where the expansion coefficients $c_{n,k}$ were calculated by Bühler et al. [16] up to the 10^{th} order in n and k. At high temperatures the spin susceptibility is small enough, therefore the sign of the temperature independent magnetic susceptibility χ_0 plays the significant role. The fitting analysis based on the HTSE is expected to be valid in the high-temperature region where the Curie-Weiss law works as well as in the lower temperature region where short-range AFM correlations occur. Thus, we carried out the HTSE fitting of the susceptibilities using equation (1) taking the susceptibility data set for the HTSE fits covering 50-300 K. Least-squares fits to the selected data set using α, χ_0, and J_1 as free parameters have been performed. The fitting analysis indicates that χ_0 is more likely to be negative than positive (except the Mn-doped sample). Figure 3.5 displays the results of the HTSE fits of the experimental susceptibility data of doped and undoped $LiCuVO_4$ and Table 3.1 summarizes the results of the HTSE fitting analyses. The HTSE describes the high-temperature susceptibilities well and is also able to capture the essence of the short-range magnetic ordering at lower temperatures. It is observed, the Curie-Weiss temperature $\theta \approx (J_1+J_2)/2k_B$[15] is negative for undoped, Zn and Co doped samples. For Mn doped sample it becomes positive.We have also fitted the susceptibility data taking into consideration the interchain exchange interactions (J_4 and J_5)[18] into the HTSE model. The fitted parameters

are shown in Table 3.2. It is also observed that the sign of $\theta \approx (J_1+J_2+J_4+2J_5)/2k_B$ value is consistent with that observed in Table 3.1.

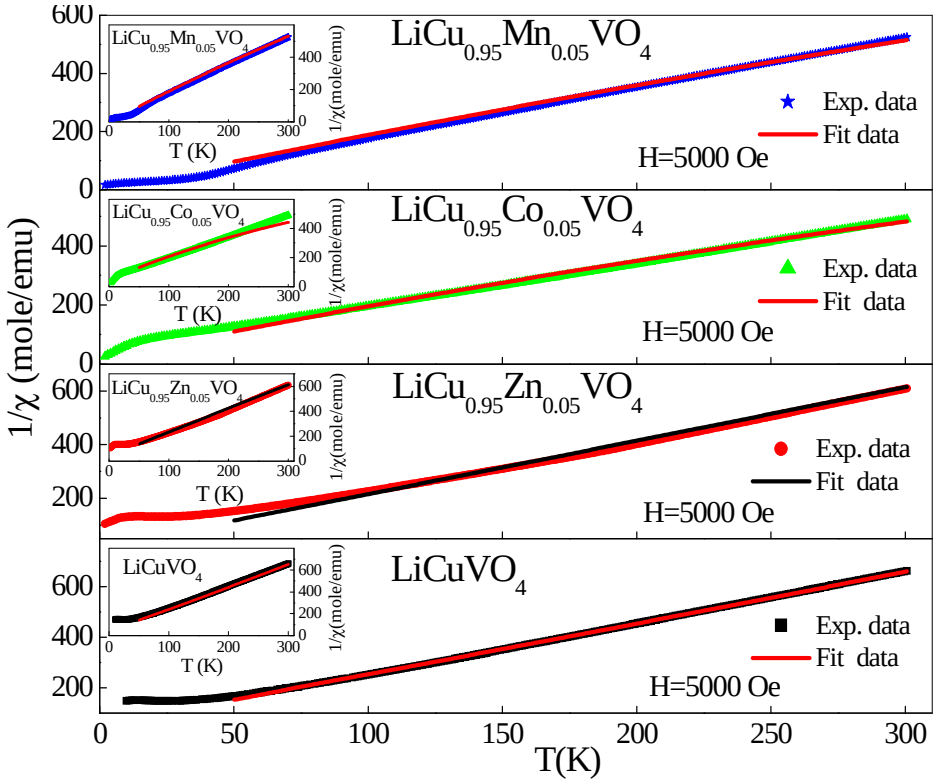

Figure 3.5: *HTSE fitting of the 1/χ(T) data of $LiCuVO_4$, $LiCu_{0.95}Zn_{0.05}VO_4$, $LiCu_{0.95}Co_{0.05}VO_4$ and $LiCu_{0.95}Mn_{0.05}VO_4$ samples in the temperature range 50K-300K considering J_1, J_2, J_4 and J_5 interactions (Inset: HTSEfitting of samples in the temperature range 50K-300K considering J_1 and J_2 interactions).*

For undoped sample the θ value is ~-29K (Table 3.1) which is larger than that reported earlier.[15,22] But when interchain exchange interactions taken into account the observed θ value becomes consistent with those reported. The θ values thus obtained are also consistent with those obtained from Curie-Weiss fitting [Eqn.2]. From both the HTSE fitting it is observed that when Mn is doped the J_1 (nearest neighbor interaction) dominates over J_2 (next nearest neighbor interaction). On the other hand for both Zn and Co doped samples J_2 increases and J_1 decreases than those of the undoped sample. From Table 2 (when J_4 and J_5 are introduced) it is observed that for undoped sample the values of interchain exchange interactions are very small but when Zn, Co and Mn are doped the values become significant. In Zn and Co doped samples both the J_4 and J_5 are positive whereas for Mn doped sample J_4 is positive but J_5 is negative.

Table 3.2

HTSE fitting of magnetic susceptibility data of $LiCuVO_4$, $LiCu_{0.95}Zn_{0.05}VO_4$, $LiCu_{0.95}Co_{0.05}VO_4$ and $LiCu_{0.95}Mn_{0.05}VO_4$ samples in temperature range 50–300 K considering J_1, J_2, J_4 and J_5 interactions.

Sample/Parameter	$LiCuVO_4$	$LiCu_{0.95}Zn_{0.05}VO_4$	$LiCu_{0.95}Co_{0.05}VO_4$	$LiCu_{0.95}Mn_{0.05}VO_4$
J_1/k_B (K)	10.14	9.8	12.1	12.25
J_2/k_B (K)	-50.2	-70.5	-90.3	-6.06
J_4/k_B (K)	-0.36	4.20	9.32	5.20
J_5/k_B (K)	-2.15	2.42	4.01	-4.21
$\chi 0$	-3.14E-5	-2.08E-6	44E-5	27.2E-5
θ (K)	-21.29	-27.04	-32.44	3.59

Moreover, in actual case Zn is nonmagnetic and therefore with doping of Zn the magnetic moment should decrease as has been observed for the hole-doped $LiCuVO_4$.[12] But in the present investigation it has been observed that with 5% Zn doping at low temperature the magnetization value increases slightly.The increase in the magnetizationmight be due to the change of the canting angle of the Cu spins. Moreover, the spin quantum number of Co^{2+} is larger (3/2) than that of Cu^{2+} and as a matter of fact the magnetization value increases with doping of Co. Furthermore, for Co ion with S=3/2, single–ion anisotropy might also be involved for reliable quantitative analysis. But in the present investigation that can be ignored because of the very low concentration of Co. It is observed for the Mn-doped sample that θ value becomes positive (mentioned above) which is the indication of the induced ferromagnetism.

3.3.2.4 Analysis of Magnetization (M) as function of Magnetic field (H) andχ(T)*T Product as Function of Temperature

Fig. 3.6 displays the M-H hysteresis loop of all the samples at 5K. No hysteresis is observed for undoped sample. For Zn and Co doped samples small non-linearity is observed. But for Mn doped sample the value of the coercivity is significant (shown in the inset of Fig. 3.6). The changeover in response of the magnetic Cu ion with doping of Zn, Co and Mn is further illustrated in Fig. 3.7 in which the χ(T)*T product is shown as a function of temperature. For temperature independent spins, and temperatures far above the effective interaction temperature, it is found that this product is temperature independent. The χ(T)*T value changes with doping of different transition metal ions indicating essentially change of interactions among the magnetic Cu ions. At low

temperatures $\chi(T)T$ of $LiCuVO_4$ is below the other curves. This supports that the effective antiferromagnetic interaction among the magnetic Cu ions decreases slightly when Zn/Co is doped and when Mn is doped it decreases appreciably. The Mn-doped sample also shows clearly the deviation from antiferromagnetic ordering and signature of ferromagnetism.

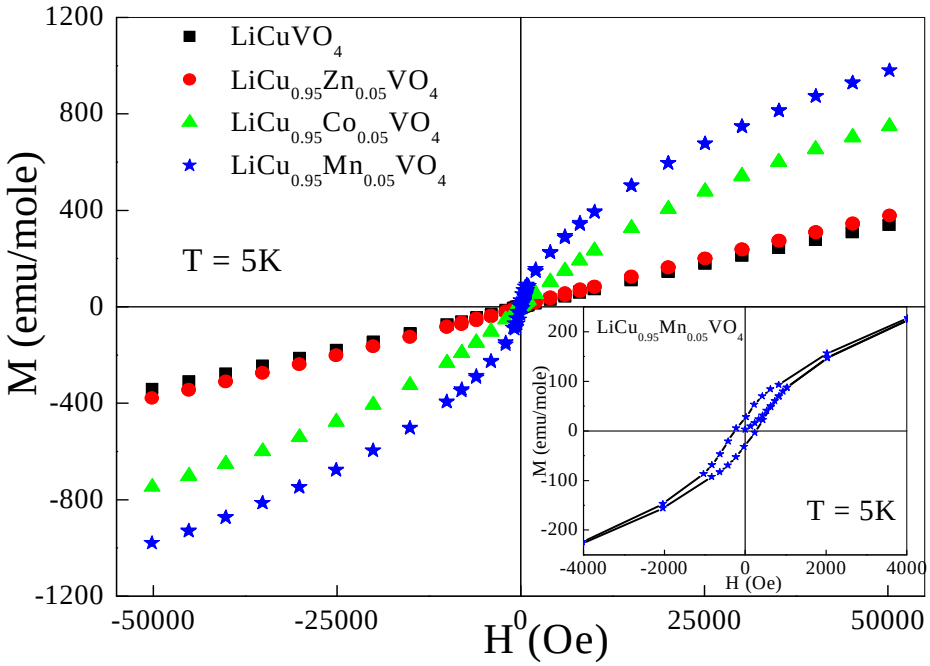

Figure 3.6: *Variation of magnetization with magnetic field (-5T to +5T) of $LiCuVO_4$,$LiCu_{0.95}Zn_{0.05}VO_4$, $LiCu_{0.95}Co_{0.05}VO_4$ and $LiCu_{0.95}Mn_{0.05}VO_4$samples.(Inset: Extended view of $LiCu_{0.95}Mn_{0.05}VO_4$ around the hysteresis loop).*

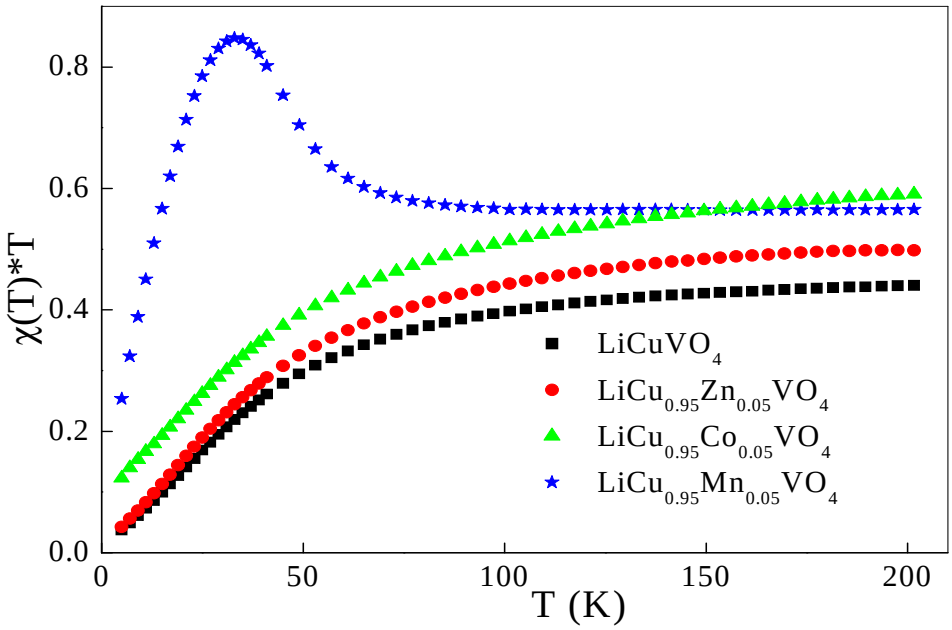

Figure 3.7: *$\chi(T)*T$ as a function of temperature of $LiCuVO_4$, $LiCu_{0.95}Zn_{0.05}VO_4$, $LiCu_{0.95}Co_{0.05}VO_4$ and $LiCu_{0.95}Mn_{0.05}VO_4$ samples at 5000 Oe.*

Furthermore, the d(χT)/dT is known as the 'Fisher specific heat' and is commonly used to determine the Curie temperature, T_c.[23-25]But the d(χT)/dT vs. T plot lack a peak, only hump is observed for the un-doped and Zn and Co-doped samples. Same hump like behaviour is also observed in χ(T) plot.

This is usual for low-dimensional system and is associated with the appearance of the magnetic correlation within the copper chains. But for Mn-doped sample only a kink is observed. Moreover, if in both χ(T) and χT(T) plots peak is observed then it indicates the magnetic ordering. For the un-doped, Zn and Co-doped samples neither in χ(T) plot nor in χT(T) plot any peak is observed within the measured temperature range. But in Mn-doped sample in both the curves peak is observed. All these indicate that there might be a FM ordering in this Mn-doped sample.

3.3.3 Neutron Diffraction Study

Neutron diffraction (ND) is a powerful tool to study the structural and magnetic properties of material due to the different doping and pristine sample. Mn-doped $LiVCuO_4$ induces ferromagnetism as above discussed. The origin of ferromagnetic ordering and what type of ordering e.g. long or short range that can be confirmed by Neutron diffraction pattern analysis. So, Neutron diffraction (ND) was performed on all the samples (shown in Fig. 3.8 (a) and 3.8 (b)) to obtain the insight feature of the magnetic and structural properties. The cell dimensions were refined using the program FULLPROF.[26]A full refinement was performed in the space group *Imma* by varying the positional parameters of the V and O atoms, the isotropic temperature factors of the V, Cu, and O atoms, the scale factors and the extinction parameter. The structure refinement was performed with least squares method. It is worthwhile to mention that we have taken both XRD and Neutron diffraction data for refinement, since Neutron diffraction does not provide any information regarding V ions. The results of these refinements are listed in Table 3.3.It is observed that for all the samples the lattice parameters decrease as the temperature decreases. There is no indication of a structural phase transition down to 5K. Thus the temperature does not cause any significant change in the crystal structure. Moreover, no superlattice peak is observed at the low temperature neutron diffraction data and hence there is no indication of the magnetic transition. Therefore, the FM ordering observed in the magnetization data for the Mn-doped sample is the short-range ordering only. It is also observed with doping the lattice parameters increase. The

parameters 'a' and 'b' increase from $LiCuVO_4$ to Zn-doped sample through Co and Mn-doped. On the other hand c parameter is maximum for Mn-doped sample.

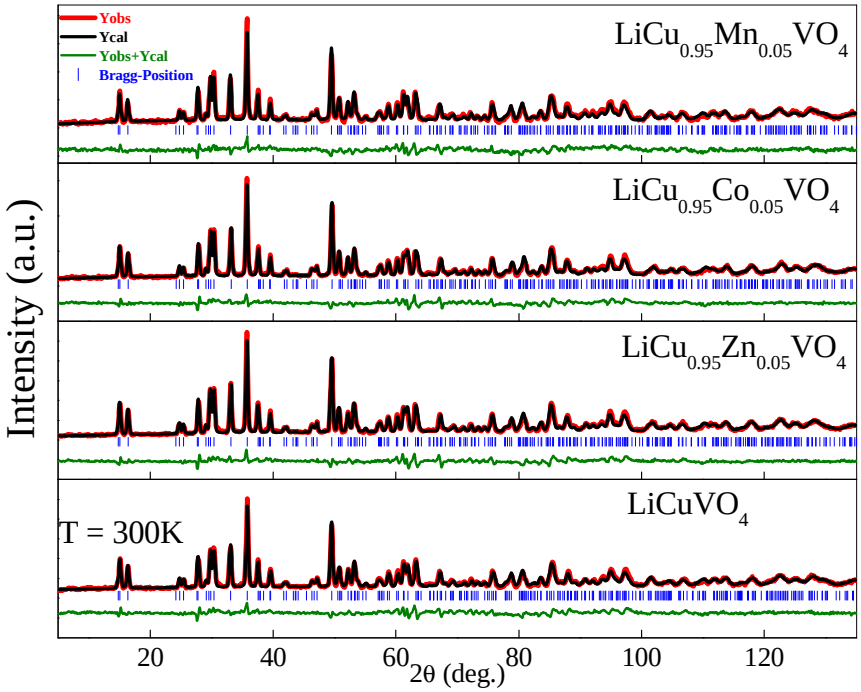

(a)

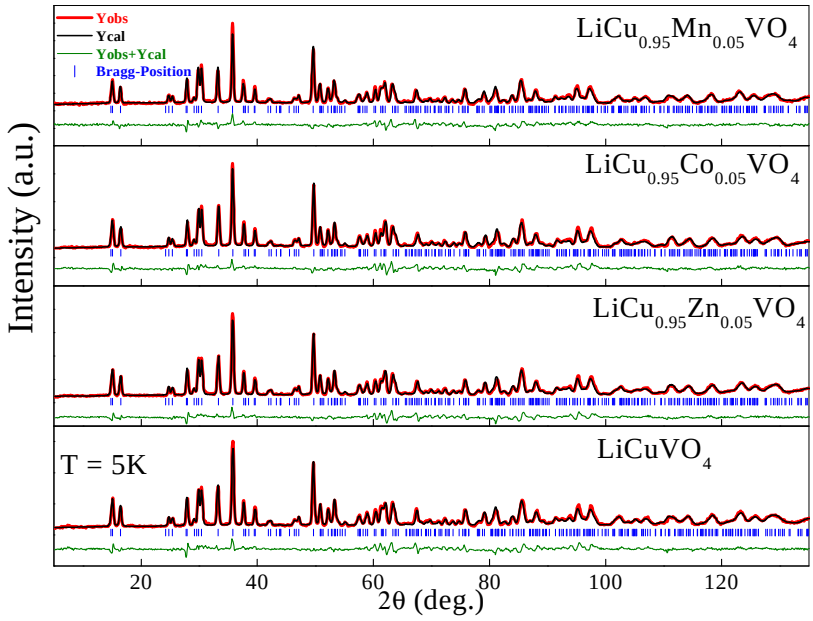

(b)

Figure 3.8: *Neutron diffraction pattern of $LiCuVO_4$, $LiCu_{0.95}Zn_{0.05}VO_4$, $LiCu_{0.95}Co_{0.05}VO_4$ and $LiCu_{0.95}Mn_{0.05}VO_4$ samples at (a) 5 K and (b) 300 K.*

Table 3.3: *Structural parameters (lattice parameters, bond lengths) of $LiCuVO_4$, $LiCu_{0.95}Zn_{0.05}VO_4$, $LiCu_{0.95}Co_{0.05}VO_4$ and $LiCu_{0.95}Mn_{0.05}VO_4$ samples obtained from Reitveld refinement. The structural data have been refined with space group Imma, Li (4d) (1/4 1/4 3/4); Cu (4a) (0 0 0); V (4e) (0 1/4 z); O1(8h)(0 y z); O2(8i)(x 1/4 z).*

Sample/ Parameter	$LiCuVO_4$ 300K	$LiCuVO_4$ 5K	$LiCu_{0.95}Mn_{0.05}VO_4$ 300K	$LiCu_{0.95}Mn_{0.05}VO_4$ 5K	$LiCu_{0.95}Co_{0.05}VO_4$ 300K	$LiCu_{0.95}Co_{0.05}VO_4$ 5K	$LiCu_{0.95}Zn_{0.05}VO_4$ 300K	$LiCu_{0.95}Zn_{0.05}VO_4$ 5K
a (Å)	5.6517(5)	5.6522(6)	5.6582(6)	5.6582(4)	5.6595(4)	5.6561(4)	5.6594(5)	5.6544(4)
b (Å)	5.8001(5)	5.7938(6)	5.8070(6)	5.8025(4)	5.8098(4)	5.7997(4)	5.8109(5)	5.7995(4)
c (Å)	8.7453(7)	8.6958(8)	8.7484(8)	8.6991(6)	8.7153(7)	8.6682(6)	8.7289(7)	8.6769(6)
Volume	286.676 (0.043)	284.767 (0.048)	287.446 (0.050)	285.605 (0.037)	286.562 (0.038)	284.348 (0.037)	287.061 (0.040)	284.537 (0.035)
V (4 e) z	0.6121(4)	0.6121(4)	0.6133(3)	0.6133(3)	0.6129(4)	0.6129(4)	0.6133(3)	0.6133(3)
O (8 h) y	0.5151(9)	0.5153(9)	0.5157(10)	0.5163(7)	0.5164(7)	0.5152(7)	0.5157(8)	0.5166(6)
z	0.2744(3)	0.2732(4)	0.2744(4)	0.2731(3)	0.2733(3)	0.2724(3)	0.2735(3)	0.2729(3)
O (8 i) x	0.2356(5)	0.2348(5)	0.2347(5)	0.2344(4)	0.2364(4)	0.2364(4)	0.2362(4)	0.2358(4)
z	-0.0005(13)	0.0003(13)	0.0009(13)	0.0039(7)	- 0.0010(10)	-0.0043(9)	-0.0004(11)	0.0002(9)
Distances								
Cu–O1 (Å)	2.401(3)	2.377(4)	2.402(4)	2.378(3)	2.384(3)	2.363(3)	2.389(3)	2.370(3)
Cu–O2 (Å)	1.969(2)	1.965(2)	1.968(2)	1.966(2)	1.975(2)	1.973(2)	1.974(2)	1.970(2)
V–O1 (Å)	1.686(5)	1.686(5)	1.678(5)	1.678(4)	1.681(4)	1.686(4)	1.682(4)	1.676(3)
V–O2 (Å)	1.785(7)	1.790(7)	1.803(7)	1.816(4)	1.782(5)	1.763(5)	1.789(6)	1.789(5)

Atom	Coord	D_aver	Distort ($x10^{-4}$)	Valence	BVSum
Li	6.0	2.1301(30)	4.129	1.000	1.003(7)
Cu	6.0	2.1129(9)	93.192	2.000	2.112(5)
V	4.0	1.7357(80)	5.203	5.000	4.825(105)
O1	4.0	2.0741(43)	146.015	-2.000	1.838(59)
O2	4.0	1.9760(49)	55.556	-2.000	2.133(46)

Moreover, it is found that the V-O(1) and V-O(2) distances are changed slightly or remain constant with doping of Zn and Co. Nonetheless when Mn is doped the change in the average V-O distances is more. The possible reason for the observed ferromagnetism can be explained as The antiferromagnetic interaction between the two spin sites of a spin dimer can be written as $J_{AF}=-(\Delta e)^2/U_{eff}$, where Δe is the spin-orbital interaction energy between the two magnetic orbitals representing two spin sites and U_{eff} is the effective onsite repulsion.[9] U_{eff} is nearly constant for closely related magnetic systems. Therefore, J_{AF} is well approximated by the corresponding $-(\Delta e)^2$. The Δe is the energy difference between the bonding level and the anti-bonding level of the spin dimer.

Along the a-direction, the empty d orbital of the V atom forming the O-V-O bridge with the oxygen atoms of the Cu-O…O-Cu path interacts in-phase with both O_{2p} orbital tails of the antibonding level, thereby lowering the antibonding level.[9] Consequently the Δe is reduced in the $LiCuVO_4$. As a matter of fact the exchange interaction along a-direction is negligible compared to nearest neighbor and next nearest neighbor interactions. But with Mn doping somehow the exchange interactions are modified which in effect might be inducing the short range ferromagnetic ordering in Mn-doped sample.

3.3.4 XPS (X-Ray Photoemission Spectra) Study

To get the effect of doping on oxidation state of Cu cations in $LiCu_{1-x}M_xVO_4$ (where M= Zn, Co, Mn and x= 0.00 and 0.05), we have also investigated the X-ray photoemission spectroscopy on these systems (Fig. 3.9). The XPS data of Cu2p region of all the samples have been shown in Fig. 3.10. Cu2p region of undoped $LiCuVO_4$ sample shows main peaks around 933.5 eV and 953.4 eV which corresponds to $Cu2p_{3/2}$ and $Cu2p_{1/2}$ respectively. Peaks around 943.9 eV and 960.9 eV correspond to satellite peaks of $Cu2p_{3/2}$ and $Cu2p_{1/2,}$ respectively.

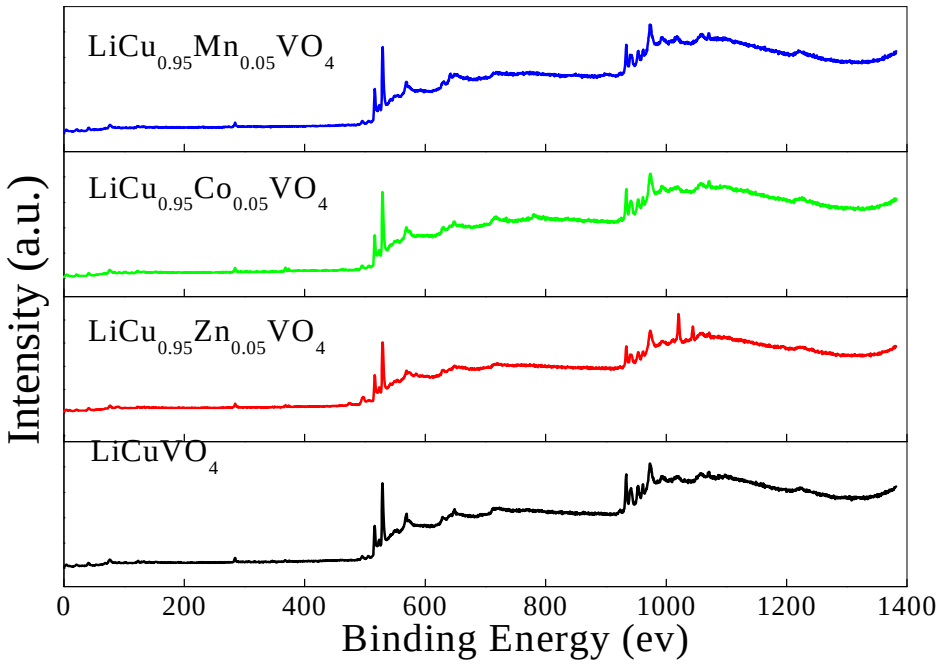

Figure 3.9: *X-ray Photoemission spectroscopy survey scan of $LiCuVO_4$, $LiCu_{0.95}Zn_{0.05}VO_4$ and $LiCu_{0.95}Co_{0.05}VO_4$ and $LiCu_{0.95}Mn_{0.05}VO_4$.*

Binding energy values match well with the Cu(II)O, which indicates the +2 oxidation state of Cu in our system. Due to doping of Zn and Co there is no significant

change observed in the binding energy of Cu cations. This means that due the doping of Zn and Co, not any appreciable change observed in the oxidation state of Cu cation. But there is small peak around 935.7 eV in Cu2p region of Mn doped $LiCuVO_4$ system. This peak clearly indicates the presence of some (very few) Cu^{3+} cations in this system. But the percentage of Cu^{3+} cations are quite low as compared to Cu^{2+} (which is due to very low doping of Mn cations) due to which no significant shift has been observed in the binding energy of Cu region. Mn2p region shows the presence of mixed Mn valences (Mn^{2+} and Mn^{3+} cations) in the Mn doped $LiCuVO_4$. This could be the case that the mixed valences of Mn cations produce the Cu^{3+} cations in this system. The Cu^{3+} is non-magnetic which in effect might decrease the next nearest neighbor anti-ferromagnetic interaction. But in the present case the Cu^{3+} cations are very less. Therefore, it deserves further study to throw light towards the actual origin of the observed ferromagnetism.

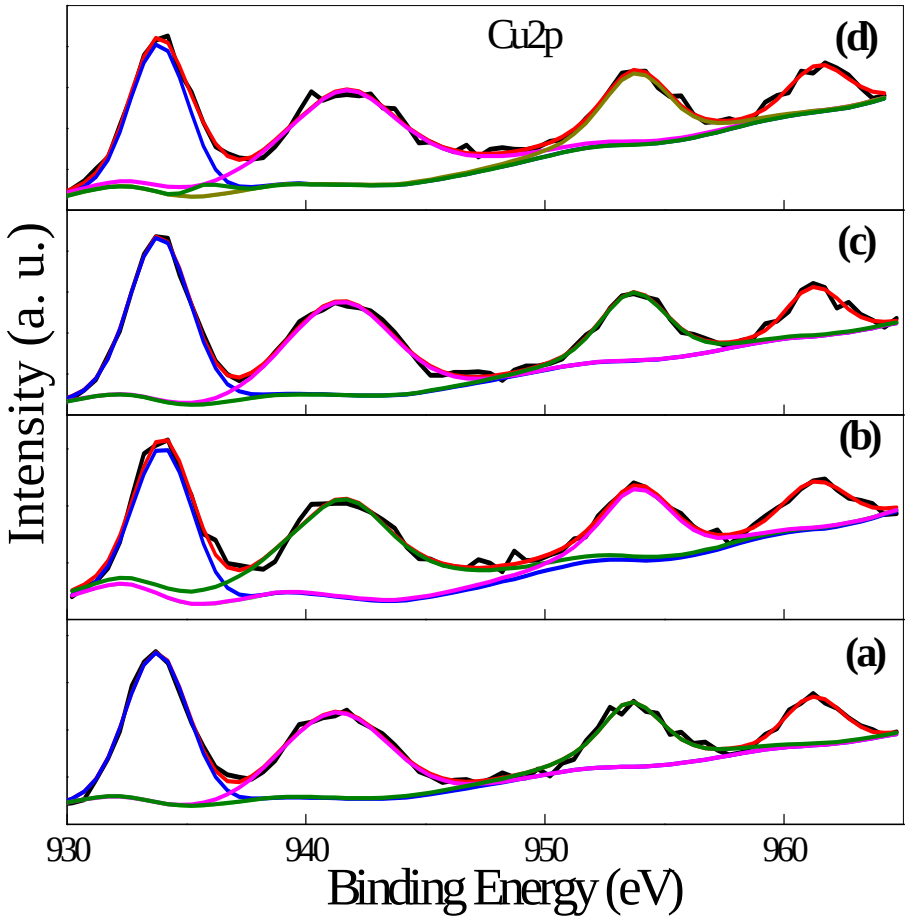

Figure 3.10: *X-ray Photoemission spectroscopic study of Cu2p of (a) $LiCuVO_4$, (b) $LiCu_{0.95}Zn_{0.05}VO_4$, (c) $LiCu_{0.95}Co_{0.05}VO_4$ and (d) $LiCu_{0.95}Mn_{0.05}VO_4$.*

3.4 Conclusion

Neutron diffraction, Magnetic properties and XPS of Zn, Co and Mn-doped $LiCuVO_4$ were investigated. When Zn and Co are doped the antiferromagnetic interaction increases. On the other hand Mn-doping induces the short range ferromagnetic ordering. It is also observed from the fitting with the HTSE model that interchain exchange interactions play significant role in doped samples. Neutron diffraction study does not show any indication of long range magnetic ordering. Neutron diffraction study also indicates that with Mn doping the V-O lengths are changed. The exchange interactions are somehow modified with Mn doping which in effect induces short range ferromagnetism. Moreover, doping of Mn on the Cu site of $LiCuVO_4$ converts very few Cu^{2+} ions into Cu^{3+} ions. Further study is required to explain the actual origin of ferromagnetism in $LiCuVO_4$ with Mn doping.

References

[1] A. Shengelaya, G. T. Meijer, J. Karpinski, Guo-meng Zhao, H. Schwer, E. M. Kopnin, C. Rossel and H. Keller, Phys. Rev. Lett. **80** 3626 (1998).

[2] S. A. Carter, B. Batlogg, R. J. Cava and J. J. Krajewski, W. F. Peck Jr., T. M. Rice, Phys. Rev. Lett. **77** 1378 (1996).

[3] A. A. Belik, M. Azuma and M. Takano, Inorg. Chem. **42** 8572 (2003).

[4] E. Dagotto and T. M. Rice, Science **271** 618 (1996).

[5] Z. Hiroi, S. Amelinckx, G. Van Tendeloo and N. Kobayashi, Phys. Rev. B. **54**15849 (1996).

[6] Y. Naito, K. Sato, Y. Yasui, Y. Kobayashi, Y. Kobayashi and M. Sato, J. Phys. Soc. Jpn. **76**023708 (2007).

[7] Ch. Kegler, N. Büttgen, H.-A. Krug von Nidda, A. Krimmel, J. Svistov, B. I. Kochelaev, A. Loidl, A. Prokofiev and W. Abmus, Eur. Phys. J B **22** 321 (2001).

[8] H. A. Krug von Nidda, L. E. Svistov, M. V. Eremin, R. M. Eremina, A. Loidl, V. Kataev, A. Validov, A. Prokofiev and W. Assmus, Phys. Rev. B **65** 134445 (2002).

[9] D. Dai, H. J. Koo and M. H. Whangbo, Inorg. Chem. **43**4026 (2004).

[10] N. Hur, S. Park, P. A. Sharma, J. S. Ahn, S. Guha and S. –W. Cheong, Nature **429** 392 (2004).

[11] M. Kenzelmann, A. B. Harris, S. Jonas, C. Broholm, J. Schefer, S. B. Kim, C. L. Zhang, S.–W. Cheong, O. P. Vajk and J. W. Lynn, Phys. Rev. Lett. **95** 087206 (2005).

[12] G. Lawes, A. B. Harris, T. Kimura, N. Rogado, R. J. Cava, A. Aharony, O. Entin-Wohlman, T. Yildrim, M. Kenzelmann, C. Broholm and A. P. Ramirez, Phys. Rev. Lett. **95** 087205 (2005).

[13] A. N. Vasil'ev, L. A. Ponomarenko, H. Manaka, I. Yamada, M. Isobe and Y. Ueda, Physica B **284**1619 (2000).

[14] B. J. Gibson, R. K. Kremer, A. V. Prokofiev, W. Assmus and G. J. McIntyre, Physica B **350**e253 (2004).

[15] H. J. Koo, C. Lee, M.-H. Whangbo, G. J. McIntyre and R. K. Kremer, Inorg. Chem. **50**3582 (2011).

[16] A. Bühler1, N. Elstner, and G. S. Uhrig, Eur. Phys. J. B **16** 475 (2000).

[17] J. Sirkar, Phys. Rev. B **81**014419 (2010).

[18] M. Enderle, C. Mukherjee, B. Fåk, R. K. Kremer, J. –M. Broto, H. Rosner, S. –L. Drechsler, J. Richter, J. Malek, A. Prokofiev, W. Assmus, S. Pujol, J. –L. Raggazzoni, H. Rakoto, M. Rheinstädter and H. M. Rønnow, Euro Phys. Letters **70** 237 (2005).

[19] S. Kumar, S. Chatterjee, K. K. Chattopadhyay and A. K. Ghosh, J. Phys. Chem., C **116** 16700 (2012).

[20] A. N. Vasil'ev, L. A. Ponomarenko, H. Manaka, I. Yamada, M. Isobe and Y. Ueda, Phys. Rev. B **64**024419 (2001).

[21] F. Du, Y. Wei, Y. Chen, F. Hu, X. Bie, C. Wang, G. Chen and G. Zou, Solid State Sci. **11** 1866 (2009**)**.

[22] H.–A. Krug von Nidda, L. E. Svistov, M. V. Eremin, R. M. Eremina, A. Loidl, V. Kataev, A. Validov, A. Prokofiev and W. Aßmus, Phys. Rev. B **65**134445 (2002).

[23] T. Aharen, J. E. Greedan, F. Ning, T. Imai, V. Michaelis, H. Zhou, C. R. Wiebe and L. M. D. Cranswick, Phys. Rev. B **80** 134423 (2009).

[24] B. Cage, B. Nguyen and N. Dalal, Solid State Commun. **119**597 (2001).

[25] Amber C. McConnell, EndritShurdha, Joshua D. Bell and Joel S. Miller, J. Phys. Chem. C **116**18952 (2012).

[26] The Rietveld Method, edited by Young R. A.; Oxford University Press